



ELSEVIER

Journal of Materials Processing Technology 103 (2000) 230–236

Journal of  
**Materials  
Processing  
Technology**

www.elsevier.com/locate/jmatprotec

# Material removal in the optical polishing of hydrophilic polymer materials

J. Sun<sup>a</sup>, L.C. Zhang<sup>a,\*</sup>, Y.-W. Mai<sup>a</sup>, S. Payor<sup>b</sup>, M. Hogg<sup>b</sup>

<sup>a</sup>*Department of Mechanical and Mechatronic Engineering, Centre for Advanced Materials Technology, The University of Sydney, Sydney, NSW 2006, Australia*

<sup>b</sup>*Eycon Lens Laboratories Pty. Ltd., 296 Burns Bay Road, Lane Cove, NSW 2066, Australia*

Received 1 December 1998

## Abstract

The optical polishing of hydrophilic polymer materials is a complex process that requires a comprehensive setting of various operating parameters. Based on a series of experimental investigations and dimensional analysis, this paper presents a simple empirical equation to evaluate material removal in the polishing of optical spherical surfaces of hydrophilic polymer materials. It is shown that the polishing load applied governs the material removal, the relative sliding velocity and the sliding distance between the workpiece and polishing tool surfaces. The equation also offers a good reference for the setting of the polishing variables. © 2000 Elsevier Science S.A. All rights reserved.

*Keywords:* Modelling; Material removal; Polishing; Polymer; Dimensional analysis

## 1. Introduction

The material removal in polishing of an optical lens is a complex process, which is particularly true for the polishing of hydrophilic polymer materials with spherical surfaces. The relative motion between the tool and the workpiece varies in a complex way, as shown in Fig. 1, and involves interactions of the workpiece material, the polishing tool, the polishing agent and the substrate. The setting of polishing parameters such as the polishing load and the combination of rotating and sliding motions significantly affect the quality of a polished surface. The optimisation of these parameters is therefore critical.

There is scant literature available on this subject, as study of the polishing of spherical surfaces of hydrophilic polymer materials is rare, although some studies have been carried out regarding the mechanical properties of this type of material [1–4]. The mechanics and mechanisms of spherical surface polishing are not yet well understood. The purpose

of this paper is to evaluate and model the material removal in the polishing of hydrophilic polymers.

## 2. Experiment

### 2.1. Details of the experimental setting

A series of polishing experiments were carried out on three typical hydrophilic polymers with hydration water contents of 38, 45 and 55% (Benz38, Benz45 and Benz55). To generate a desired optical surface (with a surface roughness of less than 150 nm) and to minimise the heat damage to the surface layer, the polishing load  $P$  and the polishing time  $\tau$  were varied over a range of  $P=2, 3, 4$  and  $5$  N, and  $\tau=10, 30, 60, 90, 120$  and  $180$  s. The polishing time is normally 60 s in actual production. In the present experiments the polishing time was extended to investigate the behaviour of the materials. The tool rotation speed  $\omega_1$  was set at 1200, 1350, 1500, 1650 and 1800 rpm, whilst the sliding angular velocity  $\omega_2$  was kept constant at 50 rpm. The polishing process was conducted in a slurry form. Loose abrasive grains ( $\text{Al}_2\text{O}_3$  particles of 0.3  $\mu\text{m}$  average diameter), suspended in oil-based polishing cream, were applied to a lap

\* Corresponding author. Fax: +61-2-9351-3760.

E-mail address: zhang@mech.eng.usyd.edu.au (L.C. Zhang)

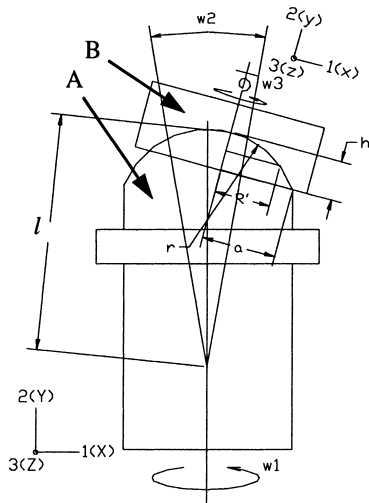


Fig. 1. A schematic diagram of the optical polishing process of spherical surfaces.

(a micro-polishing cloth). The materials were polished in a dry state, at a relative humidity of 65% and an ambient temperature of 20°C.

2.2. Observation and analysis of material removed

As assumed before, if material is removed uniformly from the polished spherical surface, a surface of radius  $r$  before polishing will become  $r + \Delta h$ , where  $\Delta h$  is the layer thickness removed, as shown in Fig. 2. Since the weight loss,  $\Delta W$ , is measured,  $\Delta h$  can be calculated easily using the following equation derived geometrically.

Since the volume of material removed is

$$\Delta V = \frac{\pi}{3} (h + \Delta h)^2 [3(r + \Delta h) - (h + \Delta h)] - \frac{\pi}{3} h^2 (3r - h) \quad (1)$$

where

$$\Delta r = \Delta h \quad (2)$$

and

$$\Delta V = \frac{\Delta W}{\rho} \quad (3)$$

then

$$\Delta h^3 + \frac{3}{2} (h + r) \Delta h^2 + 3hr \Delta h - \frac{3\Delta W}{2\pi\rho} = 0 \quad (4)$$

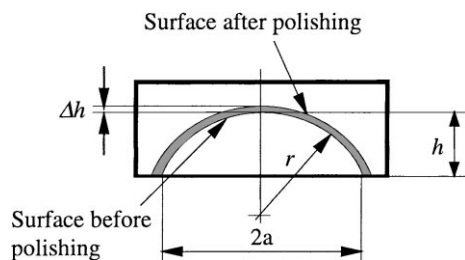


Fig. 2. Geometrical representation of layer thickness removal.

Table 1  
Density of the materials

Material	Density $\rho$ (kg/m <sup>3</sup> )
Benz38	1279
Benz45	1283
Benz55	1315

In Eq. (4), the material removed  $\Delta W$  was measured in experiments by use of an electronic balance of resolution 0.1 mg;  $h$  and  $r$ , as shown in Fig. 1, are known values ( $r=7.5$ ,  $h=3.00$  mm); the densities of the three examined materials are listed in Table 1. Thus the layer thickness removed  $\Delta h$  during a polishing process can be calculated by use of Eq. (4). Hence, the material removal rate in terms of layer thickness per unit time in metres per second or weight loss per unit time in kilograms per second can be obtained for different materials and polishing loads applied.

Figs. 3–5 show the results of the material removal experiments for the three materials. It can be seen that when the applied polishing load was greater, the material removal was faster, which indicates that the polishing load is a major dominant factor in the polishing process.

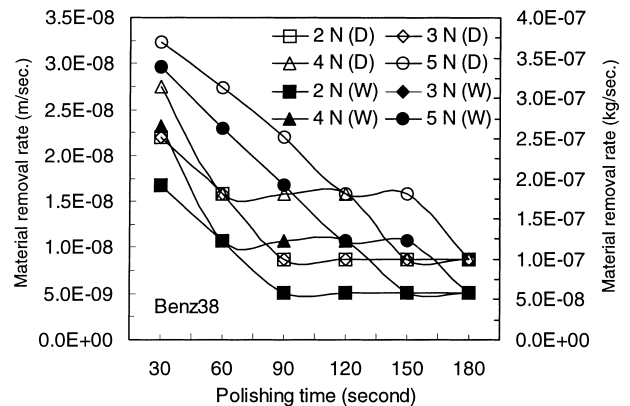


Fig. 3. Material removal response of Benz38 at different polishing loads.

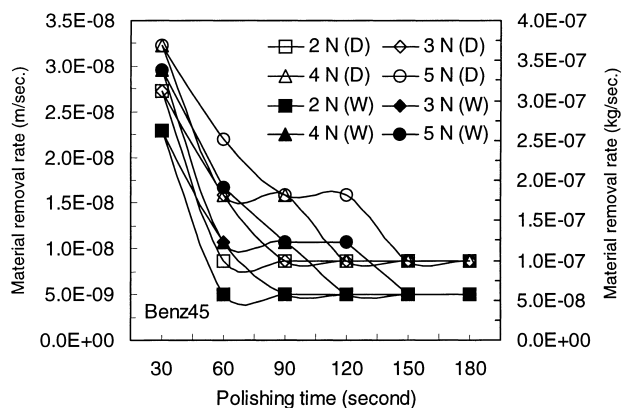


Fig. 4. Material removal response of Benz45 at different polishing loads.

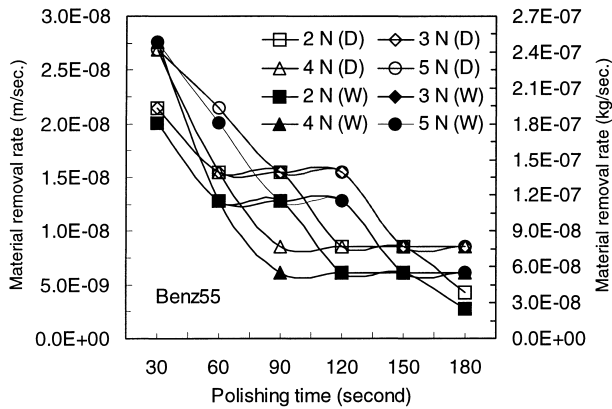


Fig. 5. Material removal response of Benz55 at different polishing loads.

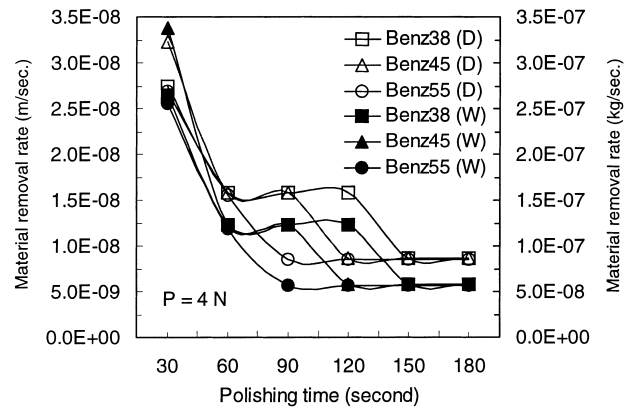


Fig. 8. Material removal response at 4 N polishing load.

Figs. 6–9 show the material removal rate of the three materials when subjected to four different polishing loads. It was found that the lesser the material hardness, the greater is the material removal rate. As shown in the figures, during the first minute of polishing, the material removal rate of Benz45 decreased relatively much more quickly, because Benz45 has the lowest hardness. This may imply that the

hardness of the material is another dominating factor in the polishing process. However, as the polishing time increases the material removal rate tends to become constant, particularly under a small polishing load. This means that as the polishing time increases the workpiece surface becomes smoother, the contact area between the surfaces of the polishing tool and workpiece increases and therefore the actual working pressure decreases and the material removal rate decreases. The above results show that effective polishing in practice is within the first minute.

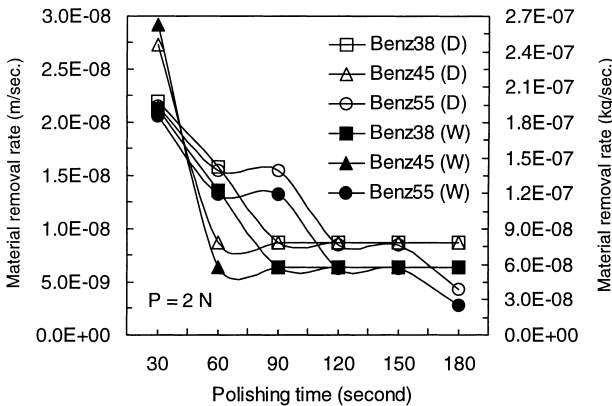


Fig. 6. Material removal response at 2 N polishing load.

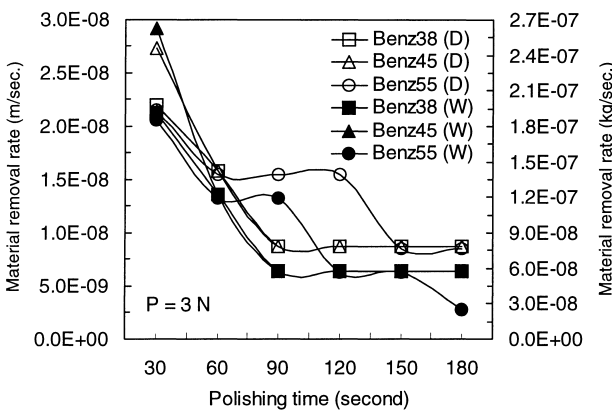


Fig. 7. Material removal response at 3 N polishing load.

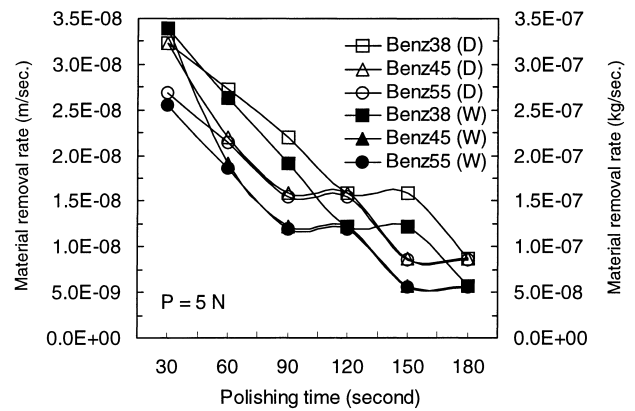


Fig. 9. Material removal response at 5 N polishing load.

### 3. Material removal evaluation

#### 3.1. The idealised model

In the polishing of a hydrophilic polymer material with a spherical surface, as shown in Fig. 1, the polishing tool A with a hemispherical end rotates with a constant angular velocity  $\omega_1$ . The workpiece B slides periodically along the hemispherical surface of A with an angular velocity  $\omega_2$ , driven by a rigid pendulum mechanism through a ‘frictionless’ ball-pin at the top centre of the workpiece. However, because of the interface friction between the tool and work-

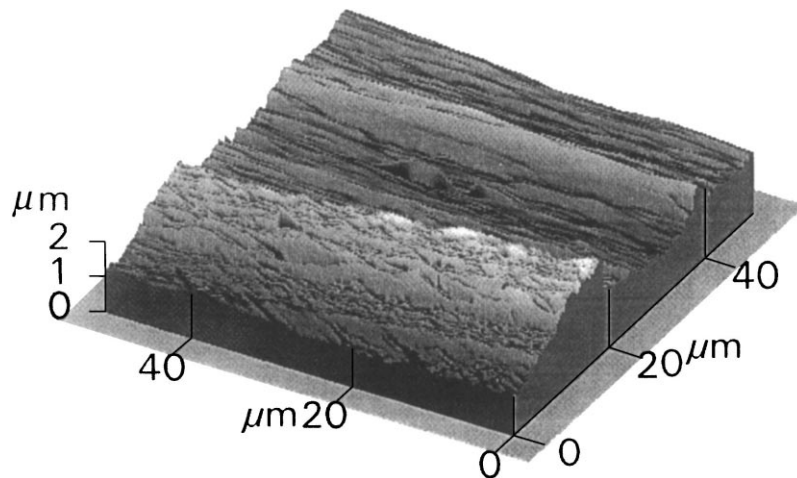


Fig. 10. Characteristics of a workpiece surface before polishing (AFM image).

piece surfaces, the workpiece also rotates about its own axis with an angular velocity  $\omega_3$ , which latter is affected by a number of parameters such as the mechanical properties of the polishing tool, the workpiece and the polishing agent, the magnitude of the polishing load applied and the angular velocities  $\omega_1$  and  $\omega_2$ . Experimental observation using a frequency analyser showed that  $\omega_3$  varies from  $0.95\omega_1$  to  $0.97\omega_1$  for the range of polishing conditions employed in production.

Only the relative sliding between the tool and workpiece surfaces contributes to material removal in polishing. In the present case, this relative sliding is characterised by: (1) the resultant sliding velocity  $v$  caused by  $\omega_2$  and  $\omega_3$ , which is generally different at different points on the workpiece surface and varies with polishing time; (2) the relative sliding distance between the tool and workpiece surfaces. According to the present microscopic examinations before and after polishing, as shown in Figs. 10–13, it was found that the material removal took place very evenly over the workpiece surface. Thus for simplicity and convenience, the real polishing mechanism illustrated in Fig. 1 can be idealised to that demonstrated in Fig. 14, where the characteristic relative sliding velocity between the workpiece and tool surfaces  $v$  is defined by the average resultant sliding velocity induced by  $\omega_2$  and  $\omega_3$ . In the idealised model,  $v$  is in a uniaxial direction and the polishing surface is considered to be flat. The apparent contact area between the workpiece and polishing tool surfaces in the model is  $A = \pi r(2a + h)$ , where  $r$  is the radius of the spherical workpiece surface. In addition, the variation of  $\omega_2$  follows a given sine function in production and  $\omega_3$  is dependent on  $\omega_1$ , as pointed out previously. Thus the product  $\omega_1\tau$  can be considered as a measure of the relative sliding distance between the tool and workpiece surfaces, where  $\tau$  is the polishing time.

With the above assumption and understanding, it is now possible to look into the relationship between material removal and the governing polishing parameters.

### 3.2. Dimensional analysis

In the idealised polishing model, variables that affect the material removal rate  $\Gamma$  are the polishing load  $P$ , the relative

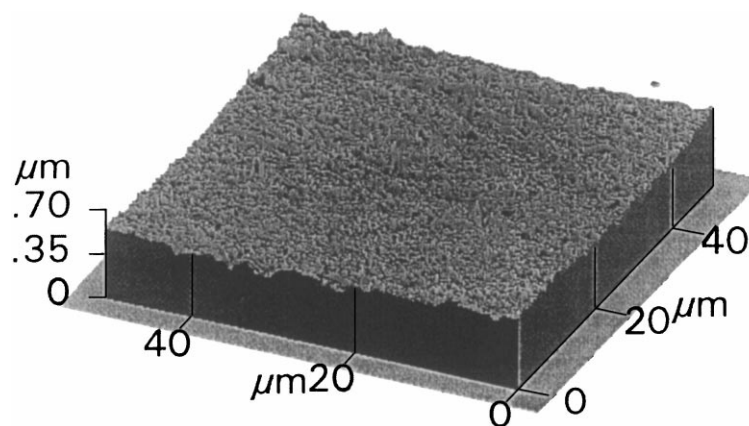


Fig. 11. Characteristics of a workpiece surface after polishing (AFM image).

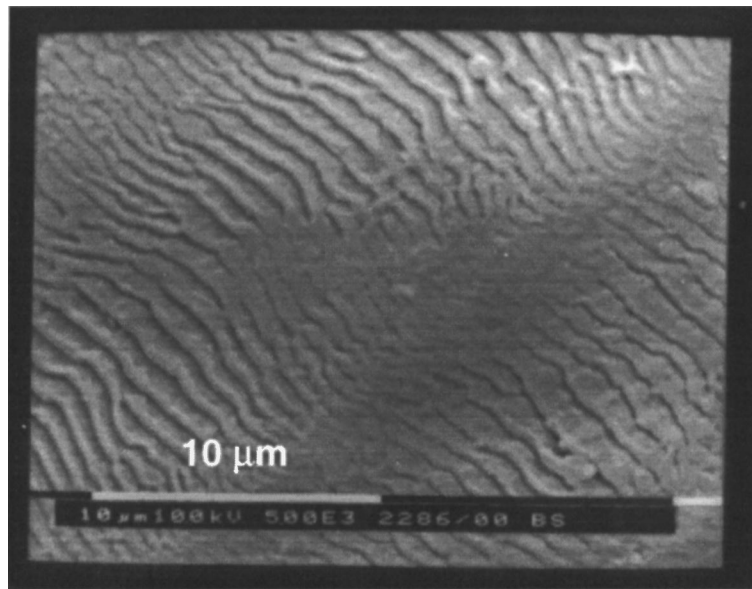


Fig. 12. Characteristics of a workpiece surface before polishing ( $\times 5000$ ) ( $\omega_1=1500$  rpm,  $P=4$  N,  $\tau=60$  s, SEM image).

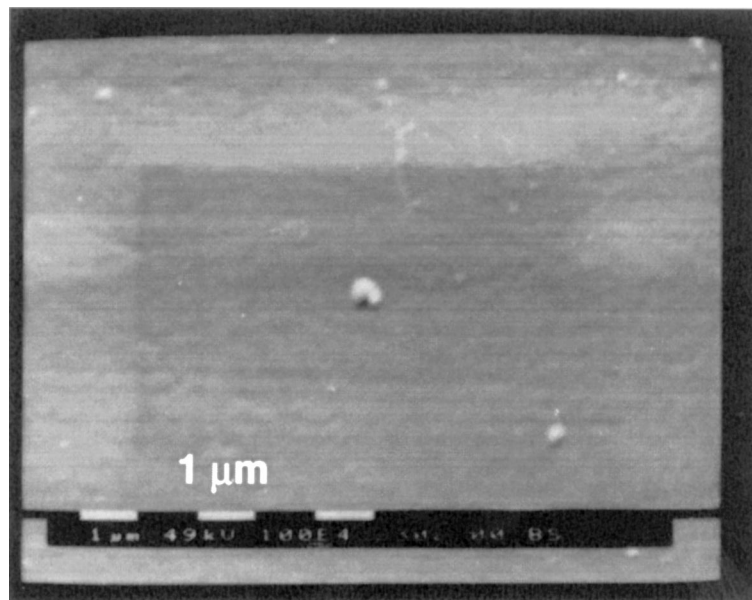


Fig. 13. Characteristics of a workpiece surface after polishing ( $\times 10\ 000$ ) ( $\omega_1=1500$  rpm,  $P=4$  N,  $\tau=60$  s, SEM image).

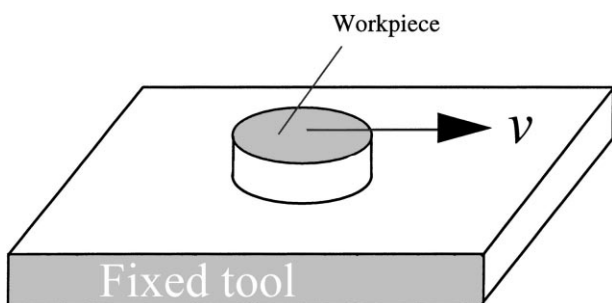


Fig. 14. The idealised model.

sliding velocity  $v$ , the apparent contact area  $A$ , the polishing time  $\tau$ , the elastic modulus of the workpiece material  $E$ , the compound elastic modulus of the polishing tool, the hardness of the workpiece material, the compound hardness of the polishing tool, the polishing temperature and the environmental humidity.

As shown in Table 2, the hardness of the hydrophilic materials used in making optical spherical surfaces does not vary greatly. The environmental humidity in actual production is maintained at a constant 65%. The compound elastic modulus of the polishing tool is also a constant in produc-

Table 2  
The mechanical properties of the materials

Material	Hardness (GPa)	Elastic modulus (GPa)
Benz38	0.144	3.180
Benz45	0.118	2.577
Benz55	0.186	3.949

tion. In addition, previous investigation of the polishing of the same types of material [4] has shown that a considerable temperature rise occurred only in the first 60 s of polishing, the temperature becoming relatively stable afterwards. At the same time, the increase of temperature increased the hardness of the workpiece material. Thus in terms of the overall material removal rate, the resultant effect of temperature rise is not considerable. All of these factors indicate that as a first approximation, the effect of temperature rise, hardness, the compound elastic modulus of the polishing tool and the environmental humidity on the material removal rate can be excluded from the formulation. Thus only the seven variables listed in Table 3 need to be considered. In Table 3, the non-dimensional velocity of relative sliding,  $v/\omega_1 R'$ , and the angular travel distance,  $\omega_1 \tau$ , have been introduced, since such introduction not only reduces the number of variables but also reflects the dependence of  $v$  on the angular velocity of the polishing tool  $\omega_1$ , which has been indicated strongly by the experimental observations reported above.

The pi theorem of dimensional analysis [5] is employed to form all of the independent non-dimensional products. In the present case, there are seven polishing variables listed in Table 3 and three primary units, i.e., mass  $M$ , length  $L$  and time  $T$ . This means that four independent non-dimensional products are required. However, as  $v/\omega_1 R'$  and  $\omega_1 \tau$  are already dimensionless, only two non-dimensional products need to be formed from the five remaining variables, with each of the products involving four of the five variables.

Table 3  
List of variables and dimensional formula

Polishing variable	Symbol of variable	Dimensional formula
Material removal rate (weight per unit time)	$\Gamma$	$MLT^{-3}$
Polishing load	$P$	$MLT^{-2}$
Elastic modulus	$E$	$ML^{-1}T^{-2}$
Relative sliding velocity	$v/\omega_1 R'$	0
Angular travel distance	$\omega_1 \tau$	0
Apparent contact area	$A$	$L^2$
Polishing time	$\tau$	$T$

Since the primary interest is in  $\Gamma$ , it should be included in only one of the products, so that it may be isolated in the final solution. In doing so, the products  $\Gamma^\alpha \tau^\beta A^\delta E^\gamma$  and  $P^a A^b \tau^c E^d$  are chosen. The exponents in these products are unknown but they must make the products dimensionless. A standard dimensional analysis using the dimensional formulae in Table 3 leads to

$$\frac{\Gamma \tau}{AE} = f\left(\frac{P}{AE}, \frac{v}{\omega_1 R'}, \omega_1 \tau\right) \tag{5}$$

with  $f$  being unrestricted. As expected, assuming that the solution can be expressed in terms of the power products of the independent non-dimensional groups, Eq. (5) can be rewritten as

$$\Gamma_0 \equiv \frac{\Gamma \tau}{AE} \sim k \left(\frac{P}{AE}\right)^\xi \left(\frac{v}{\omega_1 R'}\right)^\zeta (\omega_1 \tau)^\zeta \tag{6}$$

where  $\Gamma_0$  is the dimensionless material removal, and  $\xi$ ,  $\zeta$  and  $\zeta$  are all dimensionless constants to be determined by experiment. Eq. (6) describes the non-dimensional relationship between the level of material removal and the two most influential polishing variables, polishing load and relative sliding velocity.

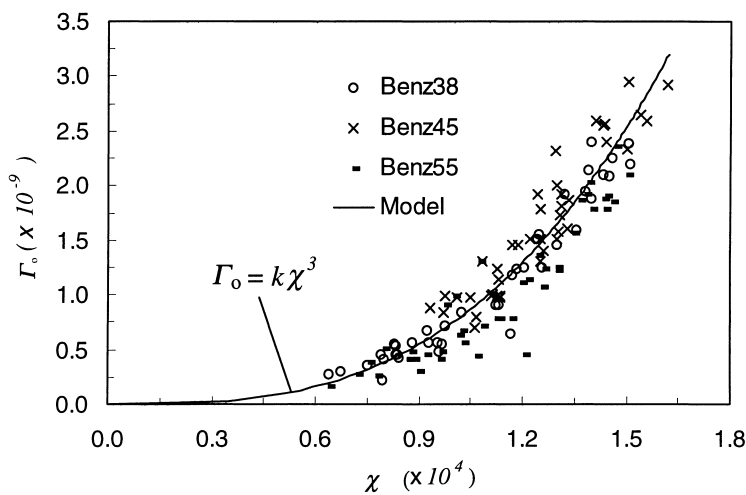


Fig. 15. The relationship between material removal and governing polishing parameters.

### 3.3. Experimental study

Using the experimental results presented in the previous sections and with the aid of multi-variable regression analysis, it was found that  $\xi$ ,  $\zeta$  and  $\zeta$  are 0.5, 1.5 and 1.0, respectively. As shown in Fig. 15, all of the experimental measurements collapse to a single curve specified by

$$\Gamma_0 = k\chi^3 \quad (7)$$

where  $k=0.75$  is a non-dimensional regression constant. A simple expansion of this equation gives rise to

$$\Gamma_0 = k \left( \frac{P}{AE} \right)^{3\xi} \left( \frac{v}{\omega_1 R'} \right)^{3\zeta} (\omega_1 \tau)^{3\zeta} \quad (8)$$

Eq. (8) represents a more general relationship between material removal and polishing conditions than that for previous polishing models. For example, Preston's model [6–9] states that

$$\left. \frac{dh(x, t)}{dt} \right| = C(x, t)P(x, t)U(x, t) \quad (9)$$

where  $h$  is the height of the surface layer that is worn away,  $C$  a proportional factor,  $P$  the apparent contact pressure between the lap and the workpiece, which is equal to the contact load divided by the apparent area of contact, and  $U$  the relative sliding speed between the lap and the workpiece, which is a special case of Eq. (8) with  $\xi = 1/3$ ,  $\zeta = 1/3$  and  $\zeta=0$ .

Fig. 15 and Eq. (8) state that material removal is an increasing function of the polishing load, the characterised relative sliding velocity and the sliding distance. This is understandable because the greater the pressure, the deeper to which the abrasives penetrate, resulting in deeper scratches and a larger volume of material removal. A higher sliding speed and a longer sliding distance should also lead to greater material removal. It is interesting to note that  $P/AE$  in Eq. (8) is a measure of strain, which means that strain plays an important role in the process of material removal.

Eq. (8) can also be used to select polishing parameters. For instance, with a given design specification for material removal, polishing load and rotational speed of the polishing tool, the polishing time required can be determined easily.

### 4. Conclusions

Based on a series of experiments and dimensional analysis, an empirical equation has been developed to evaluate the material removal process in the optical polishing of spherical surfaces of hydrophilic materials. This equation, although simple, may also be used in the polishing of other similar materials.

### Acknowledgements

The authors would like to thank the Australian Research Council and Eycon Lens Laboratories Pty. Ltd. for their financial support for this research project. They thank also the Electronics Microscopy Unit of University of Sydney for the technical support and research facilities offered to this research project.

### References

- [1] M. Ruben, *Soft Contact Lenses: Clinical and Applied Technology*, Baillière Tindall, London, 1978.
- [2] V.A. Bely, A.I. Sviridenok, M.L. Petrokovets, V.G. Savkin, *Friction and Wear in Polymer-Based Materials*, Pergamon Press, New York, 1982, pp. 3–28.
- [3] Y. Yamaguchi, *Tribology of Plastic Materials*, Elsevier, New York, 1990, pp. 1–92.
- [4] J. Sun, L.C. Zhang, Y.-W. Mai, M. Hogg, S. Payor, Material removal evaluation in the optical polishing of hydrophilic polymer materials, *Proceedings of the Ninth Annual Meeting of the American Society for Precision Engineering*, OH, USA, 1994, pp. 109–112.
- [5] E. de St Q. Isaacson, M. de St Q. Isaacson, *Dimensional Methods in Engineering and Physics: Reference Sets and the Possibilities of their Extension*, Edward Arnold, London, 1975, pp. 1–88.
- [6] F. Preston, The theory and design of plate glass polishing machines, *J. Soc. Glass Technol.* 11 (1927) 214–257.
- [7] N.J. Brown, Some speculations on the mechanisms of abrasive grinding and polishing, *Precision Eng.* 9 (3) (1987) 129–138.
- [8] K.C. Ludema, Cultural impediments to practical modelling of wear rates, *Tribological modelling for mechanical designers*, ASTM STP 1105, American Society for Testing and Materials, Baltimore, USA, 1991, pp. 180–185.
- [9] J.S. Taylor, D.M. Aikens, N.J. Brown, Framework for assessing key variable dependencies in loose-abrasive grinding and polishing, *Proceedings of the 10th Annual Meeting of the American Society for Precision Engineering*, TX, USA, 1995, pp. 260–263.